U.S. DEPARTMENT OF THE INTERIOR

U.S. GEOLOGICAL SURVEY

A Closed-Path Fourier Transform Infrared Spectrometer For Measuring Volcanic Gases

by

Kenneth A. McGee[1]

USGS Open-File Report 96-670

September 30, 1996

[1]David A. Johnston Cascades Volcano Observatory
5400 MacArthur Boulevard
Vancouver, Washington 98661

ABSTRACT. A prototype closed-path Fourier transform infrared spectrometer system, operating from battery power and without liquid nitrogen, has successfully been used for both ground-based and airborne measurements of volcanic gases. Ground-based measurements of ambient air at selected locations around the summit of Kilauea volcano revealed the presence of significant concentrations of sulfur dioxide, greater than 5 ppm in some locations, as well as excess carbon dioxide up to 50 ppm above the ambient level. Carbon monoxide was detected in one location. Airborne profiles of the volcanic plume from Pu`u `O`o on the East Rift of Kilauea by the FTIR showed levels of nearly 3 ppm SO_2 in the core of the plume. An emission rate of 2,050 t/d sulfur dioxide was calculated from the FTIR data which agrees closely with measurements by a correlation spectrometer on the same flight. This is the first measurement of a volcanic gas emission rate by an FTIR system.

INTRODUCTION

In the past twenty-five years, Fourier transform infrared (FTIR) spectroscopy has developed into a standard laboratory technique for the analysis of solids, liquids, and gases. Only recently, however, has this technique begun to be applied to volcanic gas measurements. Most volcanic gases of interest absorb infrared energy to varying degrees and are therefore potentially measurable by FTIR spectroscopy; such gases include SO_2, CO_2, CO, COS, HCl, HF, CH_4, and H_2O. Hydrogen sulfide is such a weak infrared absorber that it can be detected only if present in high concentrations (several tens of ppm or more). Diatomic gas molecules such as hydrogen, oxygen, and nitrogen do not absorb infrared radiation.

Notsu et al. (1993) used a portable FTIR spectral radiometer to remotely measure SO_2 discharging from fumaroles in the summit crater of Asama volcano from a distance of 4 km. Mori et al. (1993) used analagous instrumentation to measure the SO_2/HCl ratio in the gas plume from Unzen volcano. Very recently, Francis et al. (1995, 1996) and Mori et al. (1995) report making similar measurements at Mt. Etna and Vulcano. What all of these recent studies have in common is that they utilize open-path FTIR technology whereby an FTIR spectrometer is coupled to an optical telescope and aimed at a target gas some distance away. Either infrared light from a heated filament behind the target gas (active system) or natural infrared light (passive system) is used to introduce infrared energy into the sample path. Active systems are limited in volcanic terranes by logistical considerations in positioning the light source in hazardous or inaccessible locations. The success of measurements from passive open-path systems depends heavily on a significant temperature differential existing between the background and the target gas. Both types of open-path FTIR systems produce data in concentration x pathlength units (typically ppm•m) with the actual path distance through the target gas, and therefore the absolute gas concentration, poorly known.

In contrast, the system described here utilizes a closed-path approach to measuring volcanic gases. Gas from a volcanic plume or from ambient air near a fumarole flows through an otherwise sealed gas cell. Fixed mirrors at both ends of the gas cell with a known number of reflections between them create a pathlength of known distance. Assuming the air within the gas cell is well mixed, the absolute concentration (ppm) of the target gas within

the cell can be determined fairly accurately.

Both open- and closed-path FTIR systems have advantages and limitations. While light source and intensity problems are limitations for open-path systems, a significant disadvantage for closed-path FTIR systems is that they cannot perform analyses remotely but instead must measure the sample directly. Open-path systems are also subject to some logistical limitations (transport of FTIR to suitable plume measurement site, placement of light source in potentially hazardous locations) although not as severe. Closed-path FTIR systems can be mounted in an aircraft and flown through a volcanic plume, sampling and analyzing the gases within. Under certain conditions, emission rates of some of the gases present in plumes can be determined if enough systematic traverses through the plume are made. Both open-path and closed-path FTIR systems are subject to interference from large amounts of water vapor. Because of the large number of water lines throughout the infrared spectrum, it is sometimes difficult to quantify other gas species when water is present in excess.

INSTRUMENTATION

The closed-path FTIR system used in this study was built to USGS specifications by the MIDAC Corportion (Irvine, CA). The unit is mounted in a 90 cm x 45 cm x 30 cm ambient pressure enclosure with a 1.3 cm thick aluminum plate for an optical bench. The heart of the FTIR is a plane mirror Michelson interferometer consisting of a beamsplitter, fixed mirror, and moving mirror. Resolution is step-selectable from 32 cm^{-1} to 0.5 cm^{-1}. The interferometer splits the beam of infrared radiation from a broadband light source into two paths, introduces a phase difference, then recombines the two. Light leaving the interferometer passes through the sample gas and impinges upon the detector. When infrared radiation interacts with the sample gas, chemical bonds within the molecules of sample gas begin to vibrate and cause light to be absorbed at certain characteristic frequencies depending upon the particular gaseous molecules present in the sample. The phase difference introduced by the interferometer produces a series of cosine waves at the detector. The sum of these cosine waves is called an interferogram. One cycle of the moving mirror in the interferometer, known as a scan, is enough to produce an interferogram. A typical interferogram is shown in figure 1.

The broadband light source in this FTIR is a 1660 K silicon carbide air-cooled globar. A helium neon laser is used in order to provide a wavenumber calibration standard and also to determine the position of the moving mirror. Spectral range of the instrument is 4000 - 400 cm^{-1}. The gas cell is a permanently aligned 44-meter White cell with ceramic-protected silver-coated mirrors. Large diameter (4.8 cm) inlet and outlet ports on the side of the cell allow rapid turnover of the cell volume. The detector is made of an alloy of mercury cadmium telluride and is called a MCT detector. This type of detector usually requires liquid nitrogen for cooling in order to operate with reasonably low noise levels. One innovation of the system described here is that detector cooling is accomplished through the use of a closed-cycle Stirling engine microcooler. This cooler, essentially a compression-expansion refrigerator using helium, brings the detector temperature down to 77 K in under 5 minutes eliminating the need for liquid nitrogen.

Data collection and instrument control are accomplished through the use of a notebook PC. A special docking module on the back of the PC houses the custom interface circuitry for the spectrometer. Lab Calc from Galactic Industries (Salem, NH) is the primary software package used for data collection and spectral processing. The entire FTIR system operates off of 12 volts DC with an average current drain of 5.8 amperes, excluding the notebook PC, making transportable operation from battery power possible. The system is remarkably insensitive to vibration. Total weight is approximately 22 kg.

METHODOLOGY

The transportable closed-path FTIR spectrometer described here was designed to be used either for making ground-based measurements of ambient air or airborne measurements of volcanic plumes. Ground-based measurements of ambient air require that the instrument be transported to the measurement site which can be downwind from a volcanic crater, near a fumarole, or simply in an area of suspected poor air quality. A small battery-operated blower is connected to the exhaust port of the gas cell to draw air through the cell. Tubing of sufficient length to sample the desired air mass is connected to the inlet port. Since ground-based measurements are usually unhurried, it is possible to co-add a number of successive interferometer scans in order to reduce random noise and thereby increase significantly the signal-to-noise ratio. The improvement in signal-to-noise ratio is proportional to the square root of the integration time (Hanst and Hanst, 1994). Thus, a typical measurement of 64 scans at 1 cm^{-1} resolution would take about one minute to collect and produce a signal-to-noise ratio improvement of approximately 8 over doing just one scan. This ability to co-add scans is one of the major advantages of FTIR spectroscopy over earlier technology.

Airborne plume measurements require that the FTIR instrument be installed in an aircraft and flown through a volcanic plume. Such an installation typically consists of the FTIR powered by a 12-volt deep cycle marine battery; the notebook PC for data collection and instrument control rests on the operator's lap. A large 4.8 cm diameter 2.5-meter long PVC pipe is extended outside of the aircraft into the air stream through a window or port on the fuselage. The orientation of the PVC pipe should be nearly parallel with the long axis of the aircraft; a shallow-angle PVC elbow can be used to accomplish this if necessary. Twin engine aircraft are always preferable for airborne plume measurements in order to avoid the possibility of sampling combustion products from the engine exhaust of a front-mounted single-engine aircraft. The exterior PVC pipe is connected with 4.4 cm diameter tubing to the inlet port of the gas cell. Vacuum cleaner hose is ideal for this because it is non-collapsing yet flexible. Similar tubing is connected to the outlet port of the gas cell and extended to the exterior of the aircraft through a window or port and positioned in a rear-facing direction for cell exhaust. In order to test whether pumping gas through the cell was necessary, an airborne flow test was conducted under typical conditions (120 knots true airspeed). An average flow rate of 9.5 liters/second was measured on the outlet port of the gas cell resulting in the air in the 11-liter gas cell being completely replaced every 1.16 seconds. For comparison, the air in the gas cell of the infrared analyzer (MIRAN) used at Mount St. Helens in 1980-81 was replaced every 15 s (Harris et al., 1981). The higher flow rate of the FTIR cell allows much better plume definition.

Because this FTIR is a direct sampling instrument, it must be flown directly through the volcanic plume in order to make measurements. Typically, this involves flying systematic traverses at constant speed and at fixed vertical intervals through the plume at right angles to plume trajectory. The procedure is similar to that illustrated in Casadevall et al. (1981) for making carbon dioxide plume measurements.

As discussed earlier, the output of an interferometer is the sum of a series of cosine waves corresponding to an infrared spectrum. A mathematical algorithm, called a Fourier transform function, converts this output, or interferogram, into a single beam spectrum which is essentially a plot of infrared intensity versus frequency. In FTIR spectroscopy, frequency is usually expressed as inverse centimeters (cm^{-1}) and is often referred to as wavenumbers. A typical single beam spectrum is shown in figure 2. Because there is no compensation for instrumental or environmental factors that may contribute structure to the spectrum, a reference or background spectrum must be collected and compared with the sample spectrum in order to cancel out those factors and compute the spectrum from the sample alone. Equation 1 is used to construct a standard infrared absorbance spectrum (A) from the sample (S) and reference (R) single beam spectra.

$$A = \log(R/S) \tag{1}$$

Once the sample spectrum is ratioed against the background spectrum according to equation 1, the resulting absorbance spectrum should contain only features due to the sample. A typical absorbance spectrum is shown in figure 3.

As optical absorbance is proportional to concentration according to the Beer-Lambert law, the absorbance spectrum of a sample calculated from equation 1 can be compared with a calibration standard in order to quantify the amount of a particular gas in a sample. Fortunately in FTIR spectroscopy, it is not necessary to measure actual gas standards. Digitized quantitative calibration spectra are available in a variety of resolutions so that the conditions of sample data collection can be matched. The absorbance spectrum of the standard is subtracted from the absorbance spectrum of the sample. This spectral subtraction produces a scale factor which, when multiplied by the concentration x pathlength of the calibration standard, yields the concentration x pathlength of the sample. This then is divided by the pathlength of the gas cell (44 meters in this case) to calculate the ppm concentration of the sample gas.

AMBIENT AIR MEASUREMENTS AT KILAUEA VOLCANO

Field measurements using the closed-path FTIR spectrometer were carried out in March 1994 and September 1995 at Kilauea volcano, Hawaii. The summit region of Kilauea is dominated by a large caldera dotted with small fumaroles and steam vents. A smaller and deeper pit crater, Halemaumau, lies within the southwest corner of the summit caldera. Halemaumau, with its larger and hotter fumaroles, is the major source of magmatic gas at Kilauea's summit releasing water vapor, CO_2, SO_2, and lesser amounts of other gases. Trade winds typically carry gases from the summit toward the southwest although at times southerly winds, known as kona winds, can develop.

Figure 4 shows a map view of the summit region with major FTIR measurement points labeled. The closed-path FTIR was transported to each of these sites by vehicle and set up with a blower to bring in ambient air as described earlier. A typical measurement consists of 64 co-added scans at a resolution of 1 cm^{-1}. Several measurements were made at each location. A clean air reference single-beam spectrum collected airborne at a similar elevation was used as a background spectrum to produce a final absorbance spectrum from each sample single-beam spectrum. Data for SO_2 and excess CO_2 above ambient collected during September 1995 are shown in Table 1.

Point A in figure 4 is a large thermal area northeast of Kilauea caldera known as Sulphur Bank. This area has been active for many years and contains many steam vents and solfataras. There is a small nearby circle drive for tourists. Ambient air FTIR measurements were taken at the edge of this circle drive near a steaming cairn. Sulfur dioxide concentrations measured near that point are significant and range from 1.2 to 7.5 ppm SO_2.

The range of values in Table 1 for the remaining sample points represent several measurements over a few days under varying wind conditions. For example, the lower end of the range shown for the Hawaiian Volcano Observatory parking area (point B) represents light trade wind conditions. Stronger trade winds would likely drive the values below 0.1 ppm SO_2. The middle to upper end of the SO_2 range represents measurements made during light winds from a variety of directions. The highest SO_2 values (around 0.5 ppm) were recorded under essentially stagnant wind conditions. Because the data here represent measurements on only a few days out of the year, additional measurements would likely widen the range beyond that shown in Table 1.

Point C is a hydrothermally altered area at the western edge of Halemaumau near where the SW Rift Zone intersects Halemaumau crater. It is known locally as "B-site." Besides intense local fumarolic activity, hot gases from large fumaroles deep within Halemaumau rise and spill out of the crater at this point as they begin their downwind travel toward the southwest and the Kau Desert. The ambient air at this location contains the highest concentrations of SO_2 and CO_2 above ambient measured at Kilauea with the FTIR spectrometer. In addition, it is the only location where another volcanic gas, carbon monoxide, could be detected. A value of 2.1 ppm CO was measured at this site in March 1994. Carbon monoxide was not, however, detected during the September 1995 measurements.

Also in March 1994, several FTIR measurements were made at the Halemaumau trail parking area (point D), a popular parking spot area for tourists visiting the volcano. A series of twenty measurements were made at 5 second intervals (4 scans co-added) under moderate trade wind conditions at a resolution of 1 cm^{-1}. The results, presented in Table 2, show a variation of 0.31 to 1.66 ppm SO_2 over the period of data collection with the average being 0.93 ppm SO_2. This is consistent with the September 1995 measurements shown in Table 1 and probably representative of that location.

Finally, in September 1995 the closed-path FTIR spectrometer was mounted in an automobile for a series of mobile measurements along Kilauea's Crater Rim Drive. A large-diameter PVC pipe connected with flexible tubing to the gas cell was inserted out the window on the crater side of the automobile. A small blower on the exhaust side of the gas cell was used to pull outside air through the cell. The automobile was driven at 11.2 m/s (25 mph)

from point E to point F along Crater Rim Drive while the FTIR made measurements every 5 seconds (4 scans co-added at a resolution of 1 cm^{-1}). Typical trade wind conditions were present during the measurements (3.8 m/s from 040°) making the summit plume from Kilauea easily detectable downwind along Crater Rim Drive. The results from three measurement runs are shown in figures 3A, 3B, and 3C.

AIRBORNE PLUME MEASUREMENTS AT KILAUEA

Significant quantities of gas are released from vents and other degassing sites along the East Rift Zone of Kilauea. Chief among these degassing sites is Pu`u `O`o cone which contains several vents and an active lava pond. On September 19, 1995, the closed-path FTIR spectrometer was mounted in a twin-engine aircraft and flown along the East Rift. The instrument was configured for sampling external air as described earlier. A series of measurement traverses were made across the plume about 1 km downwind from Pu`u `O`o perpendicular to plume trajectory. Eight traverses were made at 152-meter intervals through the plume from an altitude of 1829 m down to 762 m. The FTIR sample interval was 5 seconds at a resolution of 1 cm^{-1}. Four scans were co-added during each sample interval. Flying at a true airspeed of 54 m/s, 7-8 measurements were made within the plume on each traverse across the approximately 2-km wide plume. Normal trade winds with a speed of 5.65 m/s were present during the flight sequence. Background scans of clean air for reference were made earlier at an altitude of about 1200 meters over the ocean.

Figure 5 is an interpretive sketch of the Pu`u `O`o plume of September 19, 1995 with SO_2-concentration contours in ppm. The cross-section was constructed using SO_2 concentrations derived from the FTIR measurements. The plume appears symmetrical because the middle of each traverse was aligned vertically to produce the cross-section. True plume shape could be determined if GPS location data were available. The bottom of the plume intersected the ground and is inferred by the dashed lines extending from the lowest traverse. The outermost concentration contour is 0.5 ppm SO_2. The zero concentration contour, or true edge of the plume, could not be determined because SO_2 background concentrations in this area of the East Rift Zone ranged from 0.1 to 0.3 ppm probably due to the numerous scattered degassing sources. The maximum SO_2 anomaly measured in the plume was just under 3 ppm. Carbon dioxide values were too near ambient to quantify with the FTIR.

If the area between each contour line in figure 5 is integrated graphically and summed with the rest, it is possible to calculate a total plume concentration x cross section ($ppm \cdot m^2$). When this value is multiplied by the wind speed and corrected for the temperature and pressure at the elevation of the plume, an emission rate for sulfur dioxide can be determined. Such a calculation for the FTIR SO_2 data from September 19, 1995 yields an emission rate of 2,050 t/d. Correlation spectrometer (COSPEC) measurements of sulfur dioxide taken on the same flight at the same time as the FTIR measurements give a sulfur dioxide emission rate of 1,760 t/d (Tamar Elias, personnel communication). The emission rates determined by the two methods agree to better than 15% of one another. It is likely that much of the difference can be accounted for by the fact the FTIR data reduction took into account the estimated portion of the plume below the lowest traverse.

CONCLUSIONS

A closed-path Fourier transform infrared spectrometer, operating from battery power and without liquid nitrogen for detector cooling, was developed for measuring volcanic gases. This instrument, incorporating a long pathlength internal gas cell with large diameter inlet and outlet ports for rapid turnover of cell volume, was successfully used in both ground-based and airborne configurations at Kilauea volcano. Sulfur dioxide, carbon dioxide above ambient levels, and, in one instance, carbon monoxide were measured in ambient air at a variety of locations around the summit of Kilauea. These measurements confirm that sulfur dioxide is present in significant concentrations around Kilauea but is influenced greatly by wind patterns.

A series of airborne traverses with the FTIR through the plume from Pu`u `O`o on the East Rift of Kilauea revealed a peak concentration of just under 3 ppm SO_2. Because of the numerous degassing sources along the East Rift, the ambient SO_2 level was 0.1 to 0.3 ppm in this area. A cross-section of the plume with SO_2 concentration contours was produced from the FTIR data. Concentration times area calculations of the plume cross-section multiplied by wind speed along with corrections for temperature and pressure at the elevation of the plume allowed calculation of an emission rate for sulfur dioxide. The SO_2 emission rate for September 19, 1995 from FTIR measurements was 2,050 t/d which agrees closely with COSPEC measurements on the same flight. This is the first instance where FTIR technology was used to measure a volcanic gas emission rate.

Although most of the recent efforts to apply FTIR technology to the measurement of volcanic gases centers around the use of open-path systems, the results of this study indicate that closed-path FTIR systems can be utilized effectively in such an application under certain conditions. This is particularly true for airborne volcanic plume measurements. This application of FTIR technology is not yet mature but it holds much promise, especially if better ways to handle the presence of water vapor can be developed.

REFERENCES

Casadevall, T.J., Johnston, D.A., Harris, D.M., Rose, W.I., Malinconico, L.L., Stoiber, R.E., Bornhorst, T.J., Williams, S.N., Woodruff, Laurel, and Thompson, J.M., 1981. SO_2 emission rates at Mount St. Helens from March 29 through December, 1980. In: P.W. Lipman and D.L. Mullineaux (Editors), The 1980 eruptions of Mount St. Helens, Washington. U.S. Geological Survey Professional Paper 1250: 193-200.

Francis, P., Maciejewski, A., Oppenheimer, C., Chaffin, C., and Caltabiano, T., 1995, SO_2:HCl ratios in the plumes from Mt. Etna and Vulcano determined by Fourier transform spectroscopy: Geophysical Research Letters, v. 22, n. 13, p. 1717-1720.

Francis, P., Chaffin, C., Maciejewski, A., and Oppenheimer, C., 1996, Remote determination of SiF_4 in volcanic plumes: A new tool for volcano monitoring: Geophysical Research Letters, v. 23, n. 3, p. 249-252.

Hanst, P.L. and Hanst, S.T., 1994, Gas measurement in the fundamental infrared region. In: Sigrist, M.W. (Editor), Air monitoring by spectroscopic techniques. John Wiley & Sons, New York: 335-470.

Harris, D.M., Sato, Motoaki, Casadevall, T.J., Rose, W.I., and Bornhorst, T.J., 1981. Emission rates of CO_2 from plume measurements. In: P.W. Lipman and D.L. Mullineaux (Editors), The 1980 eruptions of Mount St. Helens, Washington. U.S. Geological Survey Professional Paper 1250: 201-207.

Mori, T., Notsu, K., Tohjima, Y., and Wakita, H., 1993, Remote detection of HCl and SO_2 in volcanic gas from Unzen volcano, Japan: Geophysical Research Letters, v. 20, n. 13, p. 1355-1358.

Mori, T., Notsu, K., Tohjima, Y., Wakita, H., Nuccio, P.M., and Italiano, F., 1995, Remote detection of fumarolic gas chemistry at Vulcano, Italy using a FT-IT spectral radiometer: Earth and Planetary Science Letters, v. 134, p. 219-224.

Notsu, K., Mori, T., Igarashi, G., Tohjima, Y., and Wakita, H., 1993, Infrared spectral radiometer: A new tool for remote measurement of SO_2 of volcanic gas: Geochemical Journal, v. 27, p. 361-366.

FIGURE CAPTIONS

Figure 1. Typical interferogram produced by the closed-path Fourier transform infrared spectrometer.

Figure 2. Typical single-beam spectrum produced from an interferogram after application of the Fourier transform algorithm. Two single-beam spectra, one of the sample unknown and one of the background, are required to compute a standard infrared absorbance spectrum from which gas species in the sample can be quantified.

Figure 3. Partial absorbance spectrum of a Kilauea air sample from B-site showing the 1150 cm^{-1} sulfur dioxide band.

Figure 4. Map of the summit region of Kilauea showing FTIR measurement points; A is Sulphur Bank, B is the Hawaiian Volcano Observatory parking lot, C is B-site, and D is the Halemaumau public parking area. Points E and F represent the end points for a series of mobile FTIR measurements made along Crater Rim Drive. The top of the map is north.

Figure 5. Interpretive sketch of a vertical cross-section of the Pu `u `O`o plume of September 19, 1995 with sulfur dioxide concentration contours in ppm. Airborne traverses through the plume with the FTIR at altitudes of 1829, 1676, 1524, 1372, 1219, 1067, 914, and 762 m were used to construct the cross-section.

TABLE CAPTIONS

Table 1. Summary of the range of analytical results for SO_2 and CO_2 at the four sample points shown in figure 4. Values listed for CO_2 are those above the ambient level in the atmosphere.

Table 2. Sulfur dioxide measurements at the Halemaumau visitor parking area (point D on figure 4) made just before noon on March 21, 1994.

Table 3A,3B,3C. Summary of results for a series of three mobile FTIR measurement runs made along Crater Rim Drive going from point E to point F (figure 4). The results shown are for sulfur dioxide. The measurements were made under trade wind conditions (winds out of the northeast) with the FTIR mounted in an automobile traveling about 11.2 m/s. A small blower was used to pull ambient air into the gas cell from the crater side of the automobile.

Figure 1

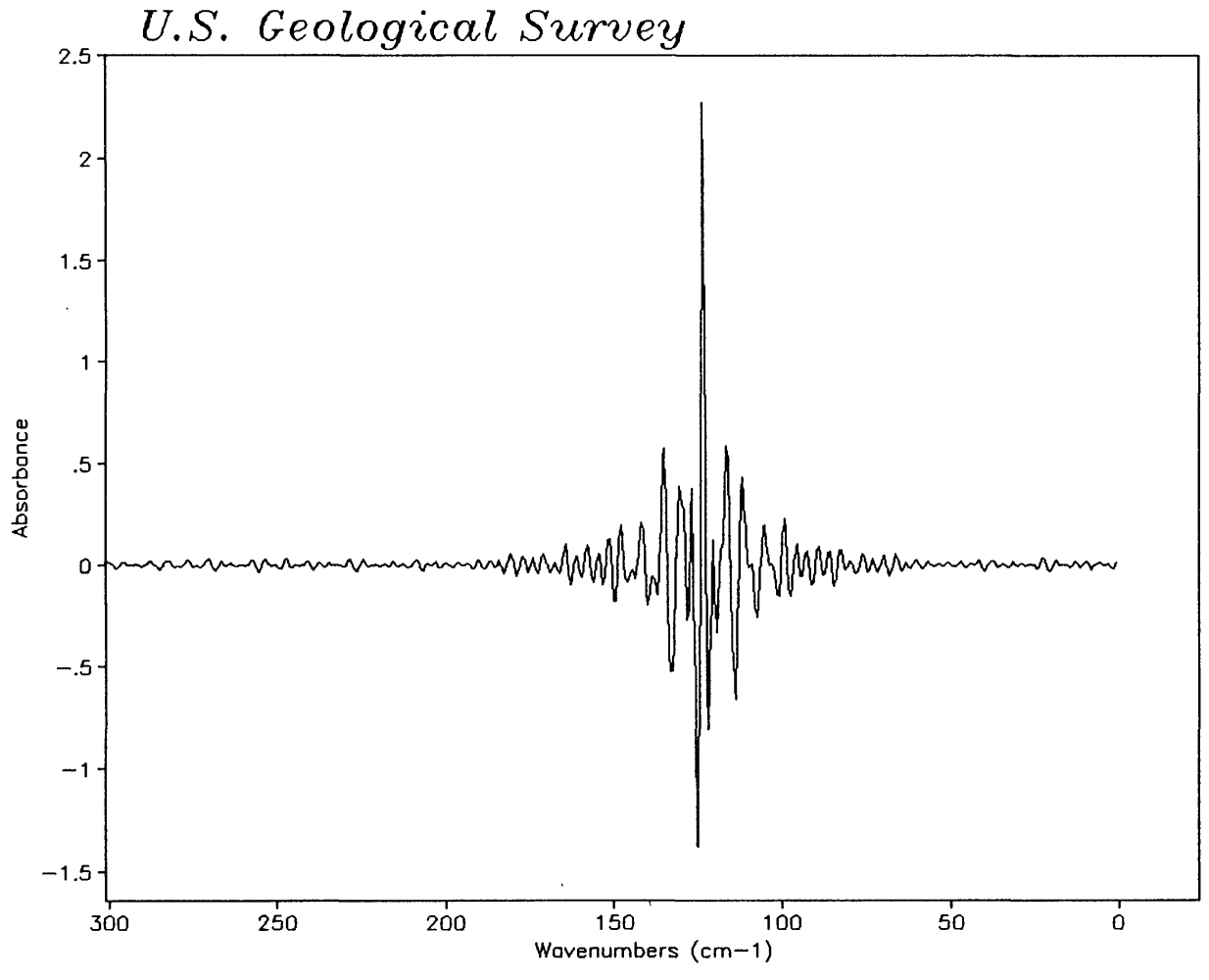
U.S. Geological Survey
2.5
2
1.5
1
.5
0
-.5
-1
-1.5
Absorbance
300
250
200
150
100
50
0
Wavenumbers (cm-1)
HVOLA7
Res= 1cm-1
09/13/95 06:20
No comment

Figure 2

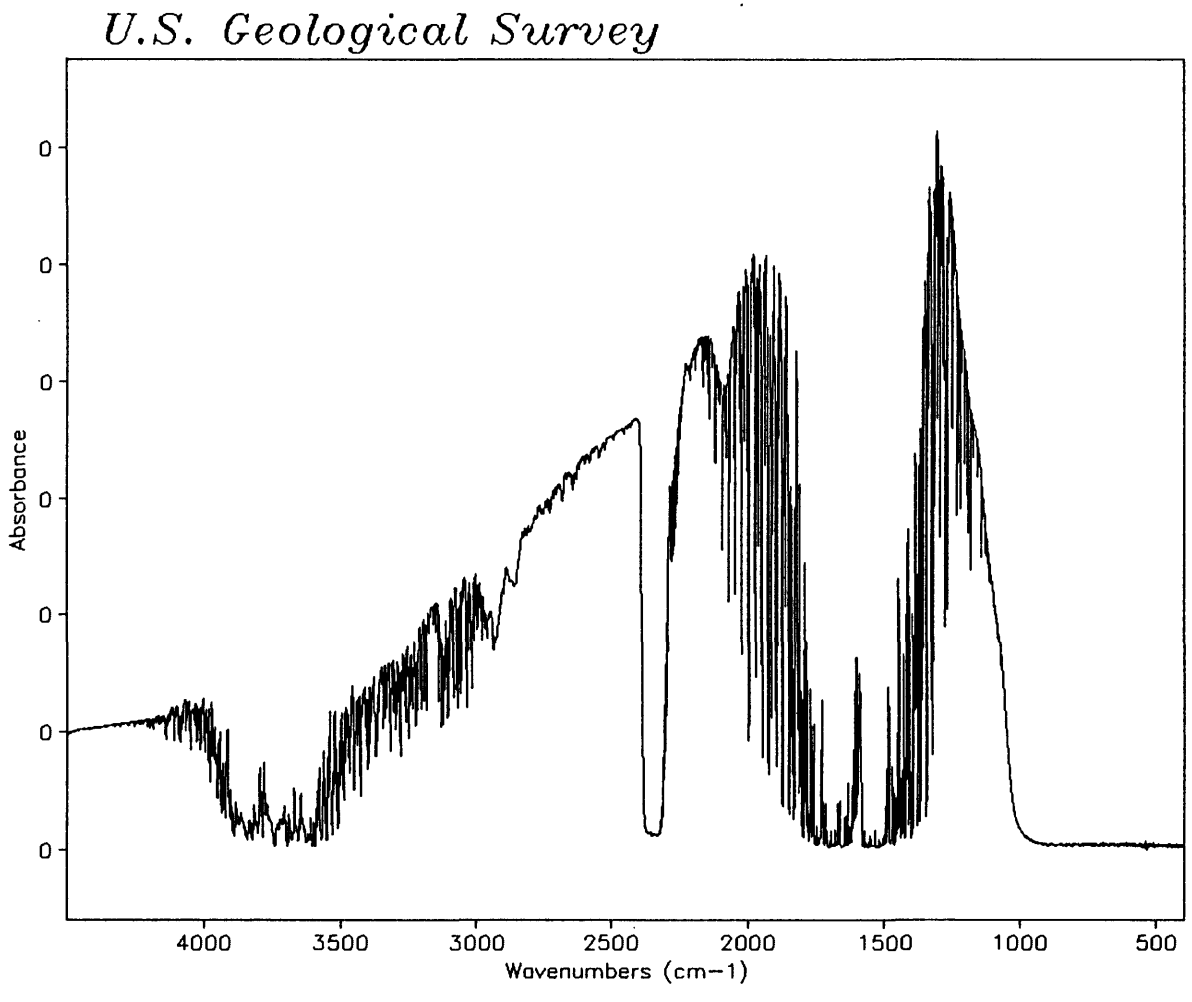
U.S. Geological Survey
Absorbance
0
0
0
0
0
0
4000
3500
3000
2500
2000
1500
1000
500
Wavenumbers (cm-1)
KILAIR8
Res= 1cm-1
09/16/95 13:31
9/16/95 using blower to pull in outside air - KiloGain=001

Figure 3

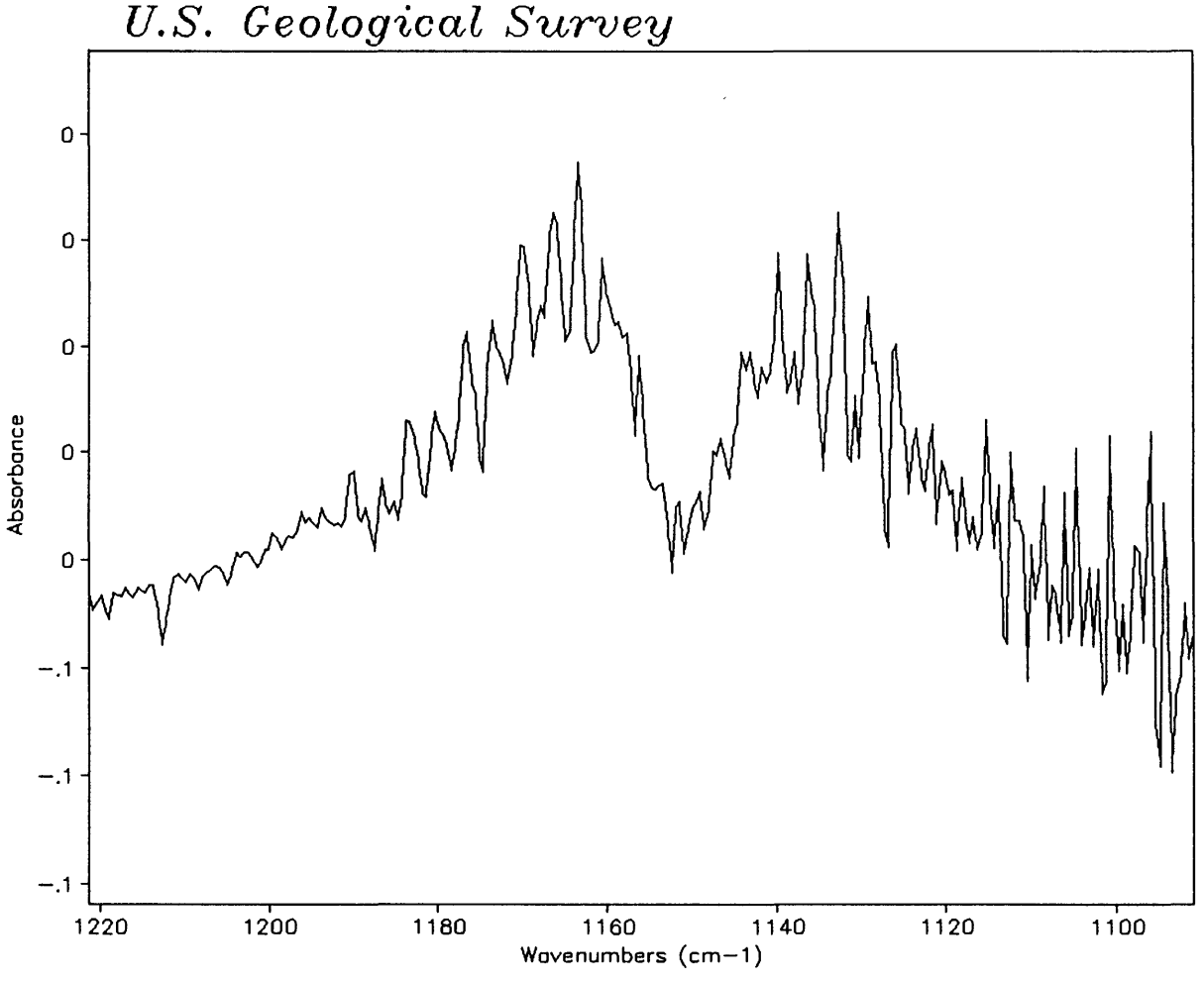
U.S. Geological Survey
Absorbance
0
0
0
0
-.1
-.1
-.1
1220
1200
1180
1160
1140
1120
1100
Wavenumbers (cm-1)
BSITA2
Res= 1cm-1
09/16/95 15:40
9/16/95 W BLOWER (6v) AT BSITE - AMBIENT
Gain=001

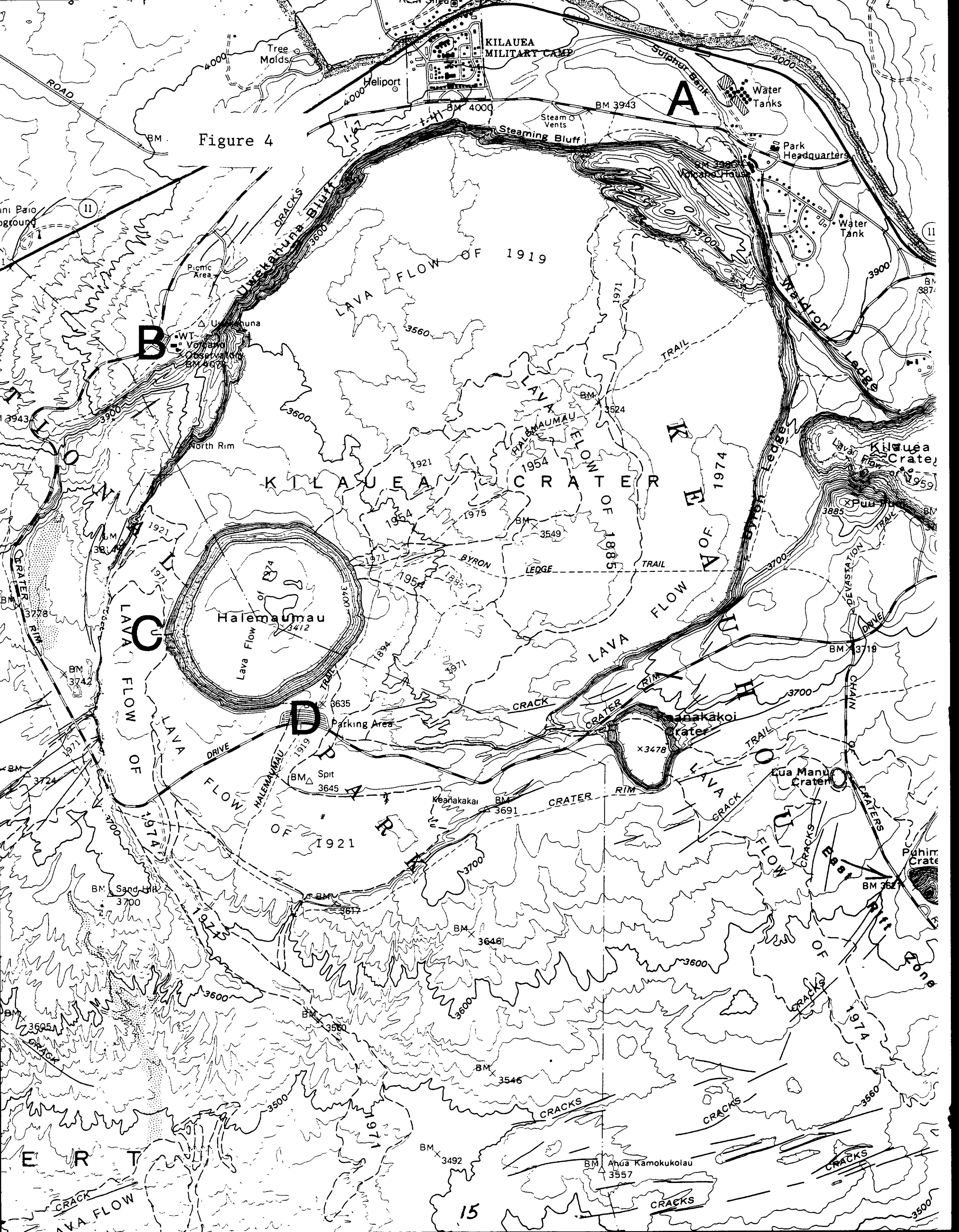
A
B
C
D
KILAUEA MILITARY CAMP
Tree Molds
Heliport
Sulphur Bank
Water Tanks
BM 4000
BM 3943
Steam Vents
Steaming Bluff
Park Headquarters
Volcano House
Water Tank
Uwekahuna Bluff
CRACKS
Picnic Area
Volcano Observatory
North Rim
LAVA FLOW OF 1919
KILAUEA CRATER
Halemaumau
LAVA FLOW OF 1974
LAVA FLOW OF 1885
Waldron Ledge
Byron Ledge
BYRON LEDGE TRAIL
HALEMAUMAU TRAIL
Kilauea Iki Crater
Puu Puai
DEVASTATION TRAIL
CHAIN OF CRATERS DRIVE
CRATER RIM DRIVE
CRATER RIM TRAIL
Parking Area
Spit
Keanakakoi Crater
Lua Manu Crater
Puhimau Crater
East Rift Zone
LAVA FLOW OF 1921
Sand Hill
Ahua Kamokukolau
KAU DESERT
HAWAII VOLCANOES NATIONAL PARK
CRACK
LAVA FLOW

Figure 4

Figure 5

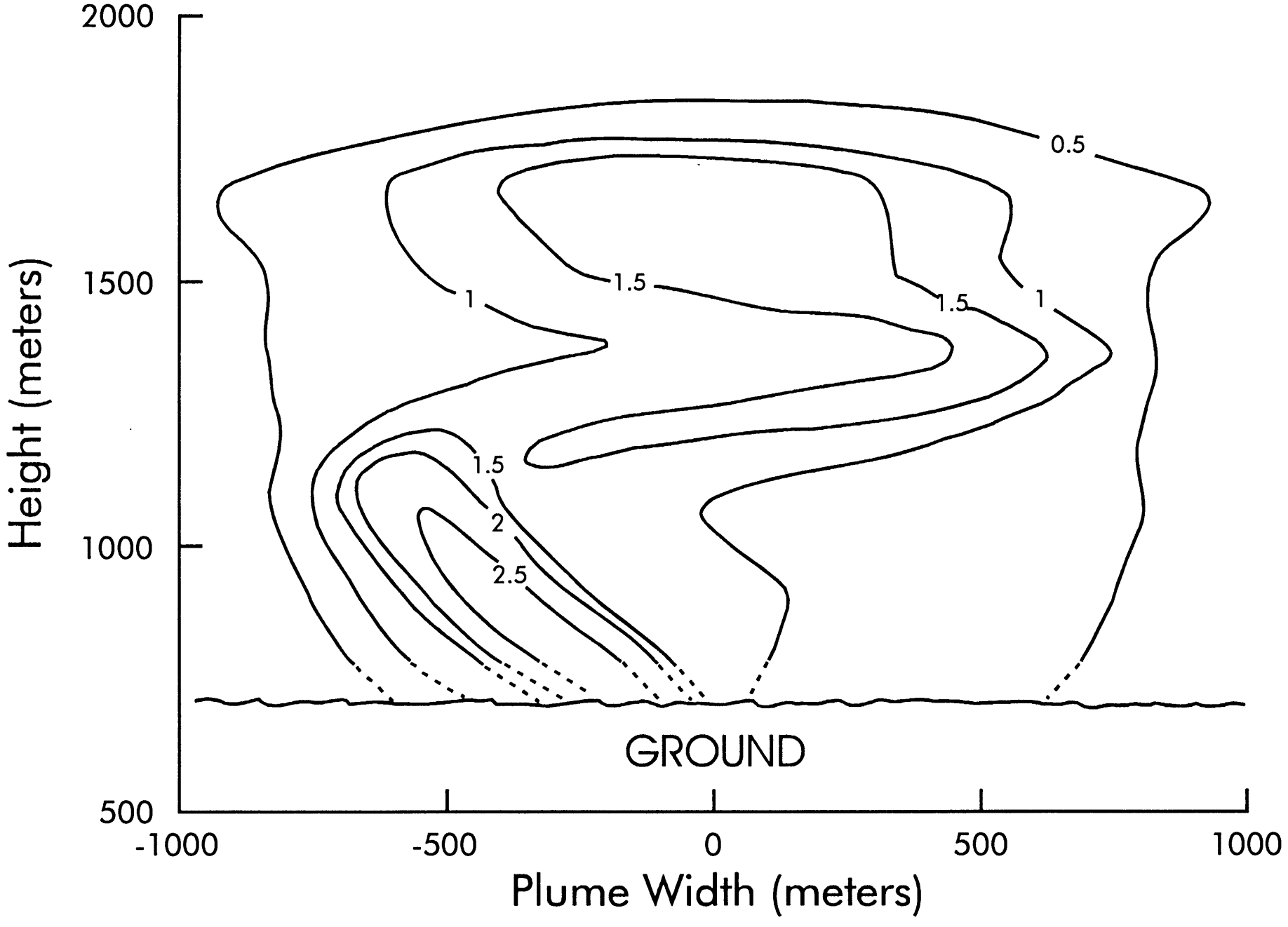
2000
1500
1000
500
Height (meters)
0.5
1
1.5
1.5
1
1.5
2
2.5
GROUND
-1000
-500
0
500
1000
Plume Width (meters)

TABLE 1
Analytical Results
September 1995

Location	SO_2 (ppm)	CO_2 (ppm)
A - Sulphur Bank	1.2 - 7.5	2 - 35
B - HVO Parking	0.1 - 0.5	1 - 4
C - B-Site	8.5 - 19.9	25 - 53
D - Hale Parking	0.6 - 1.2	12 - 42

TABLE 2
Halemaumau Visitor Parking Area
March 21, 1994
(5 Second Sampling Interval - Start Time 11:47 am HST)

Sample #	SO_2 (ppm)
PARKA1	0.86
PARKA2	0.87
PARKA3	0.92
PARKA4	0.52
PARKA5	0.31
PARKA6	0.61
PARKA7	0.95
PARKA8	0.57
PARKA9	0.79
PARKA10	1.15
PARKA11	1.28
PARKA12	0.59
PARKA13	1.46
PARKA14	0.69
PARKA15	1.66
PARKA16	0.66
PARKA17	1.49
PARKA18	0.88
PARKA19	1.30
PARKA20	1.06

AVERAGE = 0.93

TABLE 3A
Mobile FTIR Measurements Along Crater Rim Drive - RUN A
From Pt. E to Pt. F, September 20, 1995

Sample #	SO_2 (ppm)	Sample #	SO_2 (ppm)	Sample #	SO_2 (ppm)
KRIMA1	0.020	KRIMA34	1.134	KRIMA67	0.707
KRIMA2	0.051	KRIMA35	1.190	KRIMA68	0.824
KRIMA3	0.034	KRIMA36	1.349	KRIMA69	0.739
KRIMA4	0.080	KRIMA37	1.406	KRIMA70	0.676
KRIMA5	0.034	KRIMA38	1.696	KRIMA71	0.699
KRIMA6	0.065	KRIMA39	1.866	KRIMA72	0.429
KRIMA7	0.031	KRIMA40	2.401	KRIMA73	0.403
KRIMA8	0.088	KRIMA41	2.031	KRIMA74	0.540
KRIMA9	0.173	KRIMA42	1.943	KRIMA75	0.313
KRIMA10	0.091	KRIMA43	2.060	KRIMA76	0.378
KRIMA11	0.031	KRIMA44	2.006	KRIMA77	0.278
KRIMA12	0.043	KRIMA45	1.378	KRIMA78	0.321
KRIMA13	0.077	KRIMA46	1.483	KRIMA79	0.332
KRIMA14	0.043	KRIMA47	0.832	KRIMA80	0.264
KRIMA15	0.065	KRIMA48	0.716	KRIMA81	0.298
KRIMA16	0.153	KRIMA49	0.605	KRIMA82	0.358
KRIMA17	0.216	KRIMA50	0.648	KRIMA83	0.156
KRIMA18	0.222	KRIMA51	0.702	KRIMA84	0.179
KRIMA19	0.264	KRIMA52	0.287	KRIMA85	0.108
KRIMA20	0.293	KRIMA53	0.366	KRIMA86	0.116
KRIMA21	0.372	KRIMA54	0.449	KRIMA87	0.153
KRIMA22	0.432	KRIMA55	0.213	KRIMA88	0.116
KRIMA23	0.679	KRIMA56	0.267	KRIMA89	0.182
KRIMA24	0.653	KRIMA57	0.472	KRIMA90	0.114
KRIMA25	0.722	KRIMA58	0.756	KRIMA91	0.065
KRIMA26	0.881	KRIMA59	0.543	KRIMA92	0.068
KRIMA27	0.929	KRIMA60	0.653	KRIMA93	0.097
KRIMA28	1.037	KRIMA61	0.594	KRIMA94	0.085
KRIMA29	0.932	KRIMA62	0.662	KRIMA95	0.060
KRIMA30	1.139	KRIMA63	0.912	KRIMA96	0.063
KRIMA31	1.028	KRIMA64	1.006	KRIMA97	0.043
KRIMA32	1.077	KRIMA65	1.111		
KRIMA33	0.932	KRIMA66	0.841		

TABLE 3B
Mobile FTIR Measurements Along Crater Rim Drive - RUN B
From Pt. E to Pt. F, September 20, 1995

Sample #	SO_2 (ppm)	Sample #	SO_2 (ppm)	Sample #	SO_2 (ppm)
KRIMB1	0.028	KRIMB34	0.432	KRIMB67	0.418
KRIMB2	0.011	KRIMB35	0.386	KRIMB68	0.398
KRIMB3	0.011	KRIMB36	0.540	KRIMB69	0.338
KRIMB4	0.145	KRIMB37	0.679	KRIMB70	0.361
KRIMB5	0.065	KRIMB38	0.438	KRIMB71	0.327
KRIMB6	0.051	KRIMB39	1.108	KRIMB72	0.415
KRIMB7	0.023	KRIMB40	1.028	KRIMB73	0.395
KRIMB8	0.023	KRIMB41	1.134	KRIMB74	0.352
KRIMB9	0.065	KRIMB42	1.071	KRIMB75	0.364
KRIMB10	0.074	KRIMB43	1.099	KRIMB76	0.378
KRIMB11	0.080	KRIMB44	1.250	KRIMB77	0.384
KRIMB12	0.276	KRIMB45	1.048	KRIMB78	0.389
KRIMB13	0.352	KRIMB46	0.886	KRIMB79	0.335
KRIMB14	0.585	KRIMB47	0.903	KRIMB80	0.313
KRIMB15	0.287	KRIMB48	0.801	KRIMB81	0.307
KRIMB16	0.440	KRIMB49	0.653	KRIMB82	0.219
KRIMB17	0.063	KRIMB50	0.597	KRIMB83	0.264
KRIMB18	0.168	KRIMB51	0.597	KRIMB84	0.142
KRIMB19	0.466	KRIMB52	0.673	KRIMB85	0.065
KRIMB20	0.719	KRIMB53	0.753		
KRIMB21	0.753	KRIMB54	0.849		
KRIMB22	1.074	KRIMB55	0.705		
KRIMB23	1.352	KRIMB56	0.548		
KRIMB24	1.426	KRIMB57	0.716		
KRIMB25	1.080	KRIMB58	0.608		
KRIMB26	1.125	KRIMB59	0.565		
KRIMB27	0.713	KRIMB60	0.673		
KRIMB28	0.787	KRIMB61	0.463		
KRIMB29	1.310	KRIMB62	1.023		
KRIMB30	0.889	KRIMB63	0.551		
KRIMB31	0.474	KRIMB64	0.616		
KRIMB32	0.429	KRIMB65	0.526		
KRIMB33	0.415	KRIMB66	0.491		

TABLE 3C
Mobile FTIR Measurements Along Crater Rim Drive - RUN C
From Pt. E to Pt. F, September 20, 1995

Sample #	SO_2 (ppm)	Sample #	SO_2 (ppm)	Sample #	SO_2 (ppm)
KRIMC1	0.006	KRIMC34	0.889	KRIMC67	0.534
KRIMC2	0.014	KRIMC35	1.369	KRIMC68	0.440
KRIMC3	0.011	KRIMC36	1.170	KRIMC69	0.977
KRIMC4	0.026	KRIMC37	1.278	KRIMC70	0.781
KRIMC5	0.057	KRIMC38	1.341	KRIMC71	0.582
KRIMC6	0.051	KRIMC39	0.940	KRIMC72	0.412
KRIMC7	0.065	KRIMC40	1.173	KRIMC73	0.304
KRIMC8	0.028	KRIMC41	2.721	KRIMC74	0.105
KRIMC9	0.028	KRIMC42	6.145	KRIMC75	0.026
KRIMC10	0.051	KRIMC43	3.134	KRIMC76	0.619
KRIMC11	0.116	KRIMC44	0.869	KRIMC77	0.787
KRIMC12	0.082	KRIMC45	0.966	KRIMC78	0.582
KRIMC13	0.196	KRIMC46	0.670	KRIMC79	0.804
KRIMC14	0.139	KRIMC47	0.693	KRIMC80	0.307
KRIMC15	0.139	KRIMC48	0.599	KRIMC81	0.577
KRIMC16	0.506	KRIMC49	0.659	KRIMC82	0.619
KRIMC17	0.409	KRIMC50	0.665	KRIMC83	0.483
KRIMC18	0.616	KRIMC51	0.651	KRIMC84	0.335
KRIMC19	0.957	KRIMC52	0.568	KRIMC85	0.284
KRIMC20	0.892	KRIMC53	0.591	KRIMC86	0.122
KRIMC21	1.059	KRIMC54	0.545	KRIMC87	0.006
KRIMC22	1.341	KRIMC55	0.506	KRIMC88	0.037
KRIMC23	1.176	KRIMC56	0.545	KRIMC89	0.045
KRIMC24	0.898	KRIMC57	0.520		
KRIMC25	0.506	KRIMC58	0.540		
KRIMC26	0.591	KRIMC59	1.077		
KRIMC27	1.256	KRIMC60	0.795		
KRIMC28	0.531	KRIMC61	1.409		
KRIMC29	0.653	KRIMC62	1.122		
KRIMC30	0.634	KRIMC63	0.906		
KRIMC31	0.750	KRIMC64	0.764		
KRIMC32	0.724	KRIMC65	0.807		
KRIMC33	0.710	KRIMC66	0.503		